

Microscopic Theory for the Diffusion of an Active Particle in a Crowded Environment

Pierre Rizkallah,¹ Alessandro Sarracino², Olivier Bénichou,³ and Pierre Illien¹

¹*Sorbonne Université, CNRS, Laboratoire de Physico-Chimie des Électrolytes et Nanosystèmes Interfaciaux (PHENIX), 4 Place Jussieu, 75005 Paris, France*

²*Dipartimento di Ingegneria, Università della Campania “Luigi Vanvitelli”, 81031 Aversa (CE), Italy*

³*Sorbonne Université, CNRS, Laboratoire de Physique Théorique de la Matière Condensée (LPTMC), 4 Place Jussieu, 75005 Paris, France*

 (Received 9 July 2021; accepted 13 December 2021; published 19 January 2022)

We calculate the diffusion coefficient of an active tracer in a schematic crowded environment, represented as a lattice gas of passive particles with hardcore interactions. Starting from the master equation of the problem, we put forward a closure approximation that goes beyond trivial mean field and provides the diffusion coefficient for an arbitrary density of crowdiers in the system. We show that our approximation is accurate for a very wide range of parameters, and that it correctly captures numerous nonequilibrium effects, which are the signature of the activity in the system. In addition to the determination of the diffusion coefficient of the tracer, our approach allows us to characterize the perturbation of the environment induced by the displacement of the active tracer. Finally, we consider the asymptotic regimes of low and high densities, in which the expression of the diffusion coefficient of the tracer becomes explicit, and which we argue to be exact.

DOI: [10.1103/PhysRevLett.128.038001](https://doi.org/10.1103/PhysRevLett.128.038001)

Introduction.—Many theoretical models of active particles have been introduced and studied during the past decades. They were proven to be particularly powerful to describe the dynamics of a large number of real systems, ranging from biological objects (molecular motors, bacteria, micro-swimmers, algae...) to artificial self-propelled particles such as active colloids [1,2]. Among these models, run-and-tumble particles and active Brownian particles have attracted a lot of interest: in both cases, the particles self-propel with a fixed velocity, whose orientation changes randomly either abruptly or continuously, respectively. The dynamics of isolated or noninteracting active particles has been the subject of numerous recent studies [3–11].

Beyond single-particle properties, the dynamics of active particles when they interact with each other has attracted a lot of attention, and was shown to display numerous surprising effects, such as large-scale collective motion [12], clustering, or phase separation in the absence of attractive interactions [1,13]. In addition, it is crucial to understand the interactions between active particles and complex environments. Indeed, the transport of many biological objects takes place under crowded conditions, such as motor proteins inside a cell [14] or bacteria in porous materials [15]. So far, the transport of active particles in frozen disordered environments was studied through experiments (on living [16–20] and synthetic [21] microswimmers) and theoretical approaches (essentially numerical) [4,22–32].

The case of dynamic disorder, which has received much less attention, is, however, particularly relevant, since

thermal fluctuations generally affect the environment as well as the tracer [33]. Models involving tracers in environments of mobile obstacles (Fig. 1) have therefore been employed to describe situations of biological interest [34–36]. For the case of a *passive* tracer, the celebrated theory by Nakazato and Kitahara [37] (see also Refs. [38,39]) gives an expression of the corresponding diffusion coefficient as a function of the density of crowdiers, in a continuous-time description. Because of the many-body nature of the problem, this expression is approximate but has been shown to be exact in the low and high density regimes, and offers very good quantitative estimates for arbitrary density, as soon as the environment is mobile enough [38,39]. The case of an *active* tracer in a dynamic environment has been the subject of only a few

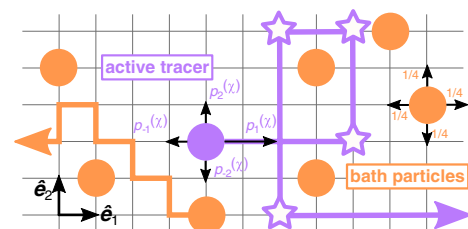


FIG. 1. An active tracer performs a persistent random walk (here, the active force initially points in direction $+e_1$, which corresponds to $\chi = 1$) in a bath of particles performing symmetric random walks (see text for notations). The orientation of the bias of the tracer changes randomly, and the reorientation events are represented by stars.

theoretical studies of particles evolving on a lattice (see, however, Ref. [40] for a very recent mode-coupling approach in continuous space), which focused mainly on the low-density limit of the problem, with a discrete-time description, with a tracer that never jumps sideways from the direction of propulsion, and with a specific dynamics [41]. Particular interactions between particles (third-neighbor exclusion) have also been studied through numerical simulations and mean-field approximations [42]. A generic analytical framework, which would allow the calculation of the diffusivity of an active tracer in a dynamic environment for a wide range of parameters, and in particular for arbitrary density, is missing. Indeed, although discrete space models for the diffusion of tracers have attracted a lot of attention and have proven particularly efficient to characterize dynamics in crowded environments, there is no continuous-time lattice model that incorporates both the effect of activity and that of crowding at arbitrary density, and that quantifies tracer-bath correlations.

In this Letter, we provide a microscopic theory for the diffusion coefficient of an active tracer in a crowded environment on a lattice, at arbitrary density and activity. Adopting a standard continuous-time dynamics and starting from the master equation describing the joint probability distribution for the position of the tracer and the configuration of its environment, we resort to a closure approximation and calculate the diffusion coefficient of the active tracer in terms of the bath density profiles, and of tracer-bath correlation functions. Importantly, in addition to the determination of the diffusion coefficient of the tracer, our approach allows us to calculate the perturbation of the environment due to the displacement of the active tracer, and the space dependence of the correlations between the tracer position and the bath occupation numbers. Finally, the expression for the diffusion coefficient becomes explicit in the low- and high-density regimes, in which we claim that our closure approximation becomes exact.

Model.—We consider an active tracer in a crowded and dynamic environment (Fig. 1). The bath particles (of density ρ), and the tracer evolve on a d -dimensional cubic lattice, whose spacing is taken equal to 1. As opposed to discrete-time descriptions [41], the system evolves here in continuous time, which is the natural and usual way to describe systems with site-blocking effects, both in one dimension as in (asymmetric) simple exclusion processes [43,44] and in higher dimensions [37–39]. Note that the dynamics of a biased tracer is known to be significantly affected by the choice of dynamics (discrete time or continuous time) [45]. The bath particles perform symmetric nearest-neighbor random walks (with characteristic time τ^*), and the tracer performs a random walk (with characteristic time τ) biased in the direction of an active force whose orientation changes randomly. The variable $\chi \in \{\pm 1, \dots, \pm d\}$ is the “state” of the tracer, i.e., the

direction in which the active force points. The tracer switches from a state χ to any other state $\chi' \neq \chi$ with rate $(\alpha/2d\tau^*)$, where α is dimensionless. The persistence time is then $\tau_\alpha = (2d\tau^*/\alpha)$. We denote by $p_\mu^{(\chi)}$ the probability for the tracer to jump in direction $\mu \in \{\pm 1, \dots, \pm d\}$ when it is in state χ . Given that the active force is in a random direction χ , we choose $p_\mu^{(\chi)} \propto \exp[F_A \mathbf{e}_\chi \cdot \mathbf{e}_\mu/2]$ with an appropriate normalization (where $\mathbf{e}_{\pm 1}, \dots, \mathbf{e}_{\pm d}$ are the lattice unit vectors and we use the notation $\mathbf{e}_{-\mu} = -\mathbf{e}_\mu$). The active force F_A is easily related to the velocity of the tracer in the absence of crowding interactions $v_0 = (p_1^{(1)} - p_{-1}^{(1)})/\tau$ [46]. The dynamics of the tracer is a lattice representation of run-and-tumble dynamics, which is a central model in the theory of active matter, and which has been widely used to describe the transport and diffusion of bacteria, see, for instance, Ref. [7]. Finally, all the particles evolve on the lattice with the restriction that there can only be one particle per site, which mimics hardcore interactions.

The state of the system at time t is described by $P_\chi(\mathbf{R}, \eta; t)$, which is the joint probability to find the tracer in state χ , at site \mathbf{R} , with the lattice in configuration $\eta = \{\eta_r\}$, where $\eta_r = 1$ if site \mathbf{r} is occupied by a bath particle and 0 otherwise. The master equation obeyed by the joint tracer-bath probability is

$$2d\tau^* \partial_t P_\chi(\mathbf{R}, \eta; t) = \mathcal{L}_\chi P_\chi - \alpha P_\chi + \frac{\alpha}{2d-1} \sum_{\chi' \neq \chi} P_{\chi'}, \quad (1)$$

where \mathcal{L}_χ is the evolution operator in state χ and is given in the Supplemental Material [47]. It accounts for the diffusion of the tracer and of the bath particles, whereas the last two terms of Eq. (1) account for the random changes in the orientation of the active force.

At $t = 0$, we assume that all the directions of the active force are equally likely, in such a way that the mean position of the tracer particle remains zero, and that at any time all states have the same probability $(1/2d)$. We are interested in the fluctuations of the tracer position along one direction, for instance, $X_t = \mathbf{X}_t \cdot \mathbf{e}_1$ (where $\mathbf{X}_t = X_t \mathbf{e}_1 + \sum_{k=2}^d X_t^{(k)} \mathbf{e}_k$). Multiplying the master equation by X_t^2 and averaging yields an expression for the time derivative of $\langle X_t^2 \rangle$, where $\langle \cdot \rangle$ denotes the average over the position of the tracer, its state, and the configuration of the lattice. The long-time diffusion coefficient of the tracer, defined as $D \equiv \lim_{t \rightarrow \infty} \frac{1}{2} (d/dt) \langle X_t^2 \rangle$, can be written under the form [47]

$$D = \frac{1}{4d\tau} \sum_\chi \sum_{\epsilon=\pm 1} \{ p_\epsilon^{(\chi)} [1 - k_\epsilon^{(\chi)}] - 2\epsilon p_\epsilon^{(\chi)} \bar{g}_\epsilon^{(\chi)} \} + \frac{2d-1}{2d} \frac{\tau^*}{\tau^2 \alpha} \sum_\chi \left\{ \sum_{\epsilon=\pm 1} \epsilon p_\epsilon^{(\chi)} [1 - k_\epsilon^{(\chi)}] \right\}^2. \quad (2)$$

This expression involves the density profiles in the frame of reference of the tracer $k_r^{(x)} = \langle \eta_{X_t+r} \rangle_\chi$ and tracer-bath cross-correlation functions $\tilde{g}_r^{(x)} = \langle \eta_{X_t+r}(X_t - \langle X_t \rangle_\chi) \rangle_\chi$, where $\langle \cdot \rangle_\chi = 2d \sum_{\mathbf{R}, \eta} \cdot P_\chi(\mathbf{R}, \eta; t)$ denotes the average conditioned on state χ [48].

Decoupling approximation.—The equations governing $k_r^{(x)}$ and $\tilde{g}_r^{(x)}$, which are obtained by multiplying the master equation [Eq. (1)], respectively, by η_{X_t+r} and $X_t \eta_{X_t+r}$, are not closed and involve higher-order correlation functions, whose evolution equations involve even higher-order correlation functions, and so on. The resulting infinite hierarchy of equations is closed by the following mean-field-type approximation: $\langle \eta_r \eta_{r'} \rangle_\chi \simeq k_r^{(x)} k_{r'}^{(x)}$ and $\langle \delta X_t \eta_r \eta_{r'} \rangle_\chi \simeq k_r^{(x)} \tilde{g}_{r'}^{(x)} + k_{r'}^{(x)} \tilde{g}_r^{(x)}$, which is obtained by writing each random variable as $x = \langle x \rangle + \delta x$ and neglecting terms of order 2 and 3 in the fluctuations. Note that this goes beyond trivial mean field, in which the mean occupation of the lattice sites would be assumed to be uniform and equal to ρ . This approximation has been successfully applied to study the velocity [49] and diffusivity [50] of a driven tracer (limit of $\alpha \rightarrow 0$) and has been shown to become exact in the low- and high-density regimes [51].

We obtain the following equations for $h_r^{(x)} \equiv k_r^{(x)} - \rho$ (defined in such a way that $\lim_{|r| \rightarrow \infty} h_r = 0$) and $\tilde{g}_r^{(x)}$ (we adopt the convention $h_0^{(x)} = \tilde{g}_0^{(x)} = 0$)

$$2d\tau^* \partial_t h_r^{(x)} = (\tilde{L}^{(x)} + \sum_\nu A_\nu^{(x)} \delta_{r, e_\nu}) h_r^{(x)} + \sum_\nu \delta_{r, e_\nu} \rho (A_\nu - A_{-\nu}) - \alpha h_r^{(x)} + \frac{\alpha}{2d-1} \sum_{\chi' \neq \chi} h_{r'}^{(\chi')}, \quad (3)$$

$$2d\tau^* \partial_t \tilde{g}_r^{(x)} = \left(\tilde{L}^{(x)} + \sum_\nu A_\nu^{(x)} \delta_{r, e_\nu} \right) \tilde{g}_r^{(x)} + \mathcal{G}^{(x)} h_r^{(x)} - \alpha \tilde{g}_r^{(x)} + \frac{\alpha}{2d-1} \sum_{\chi' \neq \chi} \tilde{g}_r^{(\chi')} + \sum_\nu \delta_{r, e_\nu} [(A_{-\nu}^{(x)} - 1) \rho (\mathbf{e}_\nu \cdot \mathbf{e}_1) - \frac{2d\tau^*}{\tau} (p_\nu^{(x)} \tilde{g}_{e_\nu}^{(x)} (h_{e_\nu}^{(x)} + \rho) - \rho p_{-\nu}^{(x)} \tilde{g}_{e_{-\nu}}^{(x)})], \quad (4)$$

where we define $A_\mu^{(x)} \equiv 1 + (2d\tau^*/\tau) p_\mu^{(x)} [1 - k_{e_\mu}^{(x)}]$, the operator $\tilde{L}^{(x)}$ acting on a test function f_r as $\tilde{L}^{(x)} f_r \equiv \sum_\mu A_\mu^{(x)} (f_{r+e_\mu} - f_r)$. The operator $\mathcal{G}^{(x)}$ is defined in Supplemental Material [47]. The sums over μ and ν implicitly run over all $2d$ directions of the lattice. Equations (3) and (4) constitute one of the main results of our Letter: within our closure approximation, these equations allow the determination of the quantities $h_r^{(x)}$ and $\tilde{g}_r^{(x)}$, and therefore of the diffusion coefficient of the

tracer through Eq. (2), for an arbitrary set of parameters, and in particular for an arbitrary density of crowders ρ .

Resolution.—The resolution of Eqs. (3) and (4) relies on the translational invariance of the system, enabling us to use Fourier transforms to invert the discrete-space differential operator. We define the following Fourier transforms, where the sum on \mathbf{r} runs over lattice sites: $H^{(x)}(\mathbf{q}; t) \equiv \sum_{\mathbf{r}} e^{i\mathbf{q}\cdot\mathbf{r}} h_{\mathbf{r}}^{(x)}(t)$ and $G^{(x)}(\mathbf{q}; t) \equiv \sum_{\mathbf{r}} e^{i\mathbf{q}\cdot\mathbf{r}} \tilde{g}_{\mathbf{r}}^{(x)}(t)$. The Fourier transforms of Eqs. (3) and (4) are given in the Supplemental Material [47]. In the stationary state, these equations are written under the form $\mathbf{M}(\mathbf{q})\mathbf{H}(\mathbf{q}) + \mathbf{R}_H(\mathbf{q}) = 0$ and $\mathbf{M}(\mathbf{q})\mathbf{G}(\mathbf{q}) + \mathbf{R}_G(\mathbf{q}) = 0$, where we define the $2d$ -dimensional vectors $\mathbf{H}(\mathbf{q}) \equiv (H^{(1)}(\mathbf{q}), H^{(-1)}(\mathbf{q}), \dots)$ and $\mathbf{G}(\mathbf{q}) \equiv (G^{(1)}(\mathbf{q}), G^{(-1)}(\mathbf{q}), \dots)$. \mathbf{R}_H depends only on $h_{e_\mu}^{(x)}$, and \mathbf{R}_G depends on $h_{e_\mu}^{(x)}$ and $\tilde{g}_{e_\mu}^{(x)}$. $\mathbf{M}(\mathbf{q})$ is a matrix such that $[\mathbf{M}(\mathbf{q})]_{\chi\chi} = -\alpha + \sum_\mu (e^{-i\mathbf{q}\cdot\mathbf{e}_\mu} - 1) A_\mu^{(x)}$ and the off-diagonal terms are all $\alpha/(2d-1)$, where we use the shorthand notation $q_\mu \equiv \mathbf{q} \cdot \mathbf{e}_\mu$. The matrix $\mathbf{M}(\mathbf{q})$ is invertible (for $\mathbf{q} \neq \mathbf{0}$), and we deduce $\mathbf{H}(\mathbf{q}) = -\mathbf{M}(\mathbf{q})^{-1} \mathbf{R}_H(\mathbf{q})$ and $\mathbf{G}(\mathbf{q}) = -\mathbf{M}(\mathbf{q})^{-1} \mathbf{R}_G(\mathbf{q})$. Then, by performing inverse Fourier transforms, we get a system satisfied by the quantities $h_\mu^{(x)}$ and $\tilde{g}_\mu^{(x)}$ [47]. This system makes it possible to calculate, within our approximation scheme, the diffusion coefficient for an arbitrary density of particles, with arbitrary values of the parameters τ , τ^* , F_A , and α .

We first give the solution for a 2D infinite lattice. We compute numerically the values of $h_\mu^{(x)}$ and $\tilde{g}_\mu^{(x)}$ in the stationary state from Eqs. (3) and (4) [47], and deduce the value of the diffusion coefficient using Eq. (2). We study the dependence of D on the density of particles on the lattice ρ , for different values of τ , τ^* , τ_α and F_A . Figure 2 displays very good agreement between Monte Carlo simulations and our decoupling approximation. As in the theory for a passive tracer [37], the accuracy of our decoupling approximation improves when the crowding environment is more mobile (typically $\tau^*/\tau \lesssim 10$) or when the dimension of the lattice is higher. In the case when there is no propulsion ($F_A = 0$), our approximation matches the result by Nakazato and Kitahara [37], which provides an explicit expression of the diffusion coefficient as a function of the density, and which is recalled in Supplemental Material [47]. Our result can therefore be seen as a generalization of this classical result on tracer diffusion in lattice gases to the case of an active particle. Note also that in the limit of $\alpha \rightarrow 0$, we retrieve the results obtained previously for the velocity and the diffusion coefficient of a passive driven tracer [50].

This calculation can easily be extended to other lattice geometries, provided that they remain translation invariant. More specifically, we consider the case of a 2D stripelike lattice (infinite in one direction and finite of width L with periodic boundary conditions in the other direction), which schematically mimics narrow channels and confined systems, and of a 3D infinite lattice (Fig. 2).

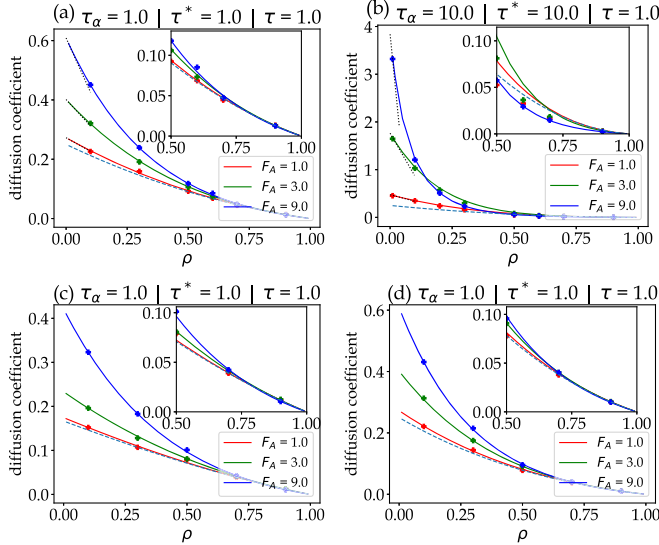


FIG. 2. Diffusion coefficient of an active tracer on a 2D lattice (a),(b), a 3D lattice (c) and a 2D capillary of width $L = 3$ (d), as a function of the density ρ , for several values of the active force F_A and the persistence time τ_α . Symbols: Monte Carlo simulations [47]. Solid lines: analytical approach [Eqs. (2), (3), and (4)]. Dotted lines: asymptotic expansion in the low-density regime. Dashed lines: case of a passive tracer [37].

Finally, we emphasize that our approach allows us to go beyond the determination of the only diffusion coefficient of the tracer, and gives access to the perturbation induced by the activity of the tracer on its environment. More precisely, we calculate the complete space dependence of the density profiles $h_r^{(\chi)}$ and of the cross-correlation functions $\tilde{g}_r^{(\chi)}$ by performing inverse Fourier transforms of $H^{(\chi)}(\mathbf{q}; t)$ and $G^{(\chi)}(\mathbf{q}; t)$ (Fig. 3). These quantities unveil the interplay between the displacement of the active tracer and the response of its environment—an aspect out-of-reach of previous descriptions [52]. In particular, we observe and quantify an accumulation of bath particles in front of the tracer and a depletion behind it. This local anisotropy of the environment of the tracer is a direct

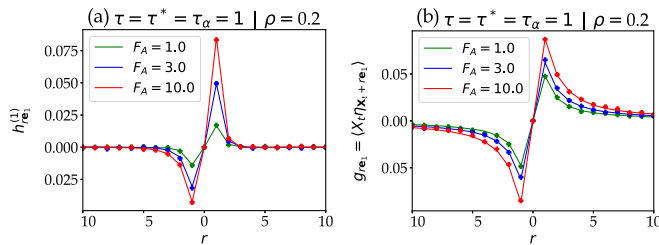


FIG. 3. (a) Density profiles (conditioned on the activity being in state $\chi = 1$) and (b) tracer-bath correlation functions (averaged on all the states) as a function of the distance to the tracer, on a 2D lattice. The values of the forces F_A , respectively, correspond to transition probabilities $p_1^{(1)} = 0.39, 0.67,$ and 0.99 . Symbols: Monte Carlo simulations. Solid lines: analytical approach.

consequence of its activity, and is fully accounted for by our approach. We provide an analytical framework to quantify the effect of active tracers on their environments, which is a key problem of active matter, with promising applications to use active tracers as microrheological probes [53].

Nonmonotony on the parameters controlling activity.— We now study the dependence of the diffusion coefficient on the persistence time τ_α . The asymptotic limits $\tau_\alpha \rightarrow 0$ and $\tau_\alpha \rightarrow \infty$ are known: when the persistence time becomes very small, the diffusion coefficient is finite and equal to that of a passive tracer [37], while in the limit of an infinitely persistent tracer, the diffusion coefficient is expected to diverge (except in the specific limit of fixed obstacles $\tau^* \rightarrow \infty$). Our analysis reveals that the diffusion coefficient can exhibit a nonmonotonic behavior between these two limits, as previously observed in the low-density limit [41]. This effect remains when $\tau^*/\tau < \infty$, but was only studied in the situation of an infinite active force, i.e., in the limit where the tracer cannot step sideways from its persistence direction [41]. Here, we go one step further and study the effect of the active force for an arbitrary density of crowders on the lattice. For a given value of ρ and τ^*/τ , the nonmonotony of the diffusion coefficient persists as long as the active force is large enough, as shown in Fig. 4. This effect results from the competition between the different timescales governing the diffusion of the tracer, and can be captured with simple analytical arguments. A phase diagram, which represents the critical value of τ^*/τ above which D becomes a nonmonotonic function of τ_α (for given density ρ and force F_A) is given in Supplemental Material (Fig. S2) [47]. We also observe a nonmonotony of the diffusion coefficient with the active force F_A , which is reminiscent of previous observations in the case of an infinitely persistent tracer [50].

Low- and high-density regimes.— Finally, as shown in Fig. 2, the decoupling approximation is accurate for the whole range of density $0 \leq \rho \leq 1$. In addition, we argue that it becomes exact in the low- and high-density regimes, that we explore here. This claim relies on the exactness of (i) the theory of Nakazato-Kitahara in the case of symmetric passive tracer [37]; and (ii) the microscopic theory of a driven passive tracer in these limits [50].

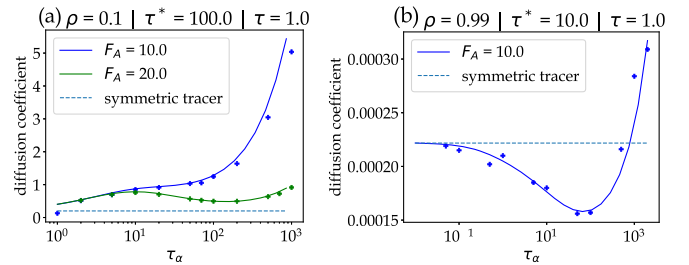


FIG. 4. Nonmonotony of D as a function of the persistence time τ_α , at density $\rho = 0.1$ (a) and $\rho = 0.99$ (b).

We expand the density profiles $h_\mu^{(x)}$ and the correlation functions $\tilde{g}_\mu^{(x)}$ in the limits of $\rho \rightarrow 0$ and $\rho \rightarrow 1$. In these limits, the diffusion coefficient of the tracer is expanded as $D = D_0 + \rho D_1 + \mathcal{O}(\rho^2)$ (respectively $D = (1 - \rho)D_1 + \mathcal{O}[(1 - \rho)^2]$), where the expressions of D_0 and D_1 (respectively \mathcal{D}_0 and \mathcal{D}_1) are expressed in terms of the leading order expressions of the coefficients $h_\mu^{(x)}$ and $\tilde{g}_\mu^{(x)}$ in the low-density (respectively high-density) limit. The latter are found to be solutions of linear systems. These solutions, together with the expansions of D , yields an *explicit* expression of the diffusion coefficient of the tracer in terms of all the parameters of the problem in these regimes (see Secs. IX and XI of the Supplemental Material [47] and Fig. 2).

In the low-density limit, this result is the continuous-time counterpart of previous low-density approaches, which relied on a specific dynamics. A comparison between the results from our decoupling approximation and the results from Ref. [41] is given in Supplemental Material [47]. Since the two dynamics are different, the two calculations of the diffusion coefficient do not match quantitatively, but display a good qualitative agreement.

These expansions give fully explicit expressions of the diffusion coefficient both in the low- and high-density regimes, which we furthermore argue to be exact. Indeed, in both limits of a driven tracer ($\tau_\alpha \rightarrow \infty$) and of a passive tracer ($\tau_\alpha \rightarrow 0$), a similar decoupling approximation was compared to exact approaches that focused (i) on the low-density limit, in which the diffusion of the tracer is seen as a succession of scattering events due to interactions with independent obstacles (at leading order in ρ) [54,55]; (ii) on the high-density limit, in which the diffusion of the tracer is mediated by the diffusion of vacancies, which explore the lattice independently (at leading order in $1 - \rho$) [56–60]. This, together with the very good agreement between the decoupling approximation and numerical results, points towards the exactness of the present approximation. Showing such exactness would require us to obtain exact results for the diffusion of an active tracer using the methods mentioned above, and this will be investigated in future work.

We hope that the present approach will allow us to establish connections with recent experimental observations on living organisms [15,61] or self-propelled particles [53] in crowded environments. Moreover, it will be technically challenging but particularly interesting to study the opposite situation of a passive tracer in a dense active environment—a situation that has recently been the object of theoretical approaches [40].

A. S. acknowledges partial support from MIUR Project No. PRIN201798CZLJ and from Program (VANviteLli pEr la RicErca: VALERE) 2019 financed by the University of Campania “L. Vanvitelli.”

[1] C. Bechinger, R. Di Leonardo, H. Löwen, C. Reichhardt, G. Volpe, and G. Volpe, *Rev. Mod. Phys.* **88**, 045006 (2016).

- [2] A. Zöttl and H. Stark, *J. Phys. Condens. Matter* **28**, 253001 (2016).
- [3] P. Romanczuk, M. Bär, W. Ebeling, B. Lindner, and L. Schimansky-Geier, *Eur. Phys. J. Special Topics* **202**, 1 (2012).
- [4] J. Tailleur and M. E. Cates, *Europhys. Lett.* **86**, 60002 (2009).
- [5] M. E. Cates and J. Tailleur, *Europhys. Lett.* **101**, 20010 (2013).
- [6] K. Malakar, V. Jemseena, A. Kundu, K. V. Kumar, S. Sabhapandit, S. N. Majumdar, S. Redner, and A. Dhar, *J. Stat. Mech.* (2018) 043215.
- [7] M. J. Schnitzer, *Phys. Rev. E* **48**, 2553 (1993).
- [8] K. Martens, L. Angelani, R. Di Leonardo, and L. Bocquet, *Eur. Phys. J. E* **35**, 84 (2012).
- [9] C. Kurzthaler, S. Leitmann, and T. Franosch, *Sci. Rep.* **6**, 36702 (2016).
- [10] U. Basu, S. N. Majumdar, A. Rosso, and G. Schehr, *Phys. Rev. E* **98**, 062121 (2018).
- [11] U. Basu, S. N. Majumdar, A. Rosso, and G. Schehr, *Phys. Rev. E* **100**, 062116 (2019).
- [12] T. Vicsek and A. Zafeiris, *Phys. Rep.* **517**, 71 (2012).
- [13] M. E. Cates and J. Tailleur, *Annu. Rev. Condens. Matter Phys.* **6**, 219 (2015).
- [14] L. Conway, D. Wood, E. Tüzel, and J. L. Ross, *Proc. Natl. Acad. Sci. U.S.A.* **109**, 20814 (2012).
- [15] N. A. Licata, B. Mohari, C. Fuqua, and S. Setayeshgar, *Biophys. J.* **110**, 247 (2016).
- [16] T. Bhattacharjee and S. S. Datta, *Nat. Commun.* **10**, 2075 (2019).
- [17] S. Makarchuk, V. C. Braz, N. A. Araújo, L. Ciric, and G. Volpe, *Nat. Commun.* **10**, 4110 (2019).
- [18] O. Sipos, K. Nagy, R. Di Leonardo, and P. Galajda, *Phys. Rev. Lett.* **114**, 258104 (2015).
- [19] M. Brun-Cosme-Bruny, E. Bertin, B. Coasne, P. Peyla, and S. Rafai, *J. Chem. Phys.* **150**, 104901 (2019).
- [20] A. Guidobaldi, Y. Jeyaram, I. Berdakin, V. V. Moshchalkov, C. A. Condat, V. I. Marconi, L. Giojalas, and A. V. Silhanek, *Phys. Rev. E* **89**, 032720 (2014).
- [21] A. Morin, N. Desreumaux, J. B. Caussin, and D. Bartolo, *Nat. Phys.* **13**, 63 (2017).
- [22] O. Chepizhko and F. Peruani, *Phys. Rev. Lett.* **111**, 160604 (2013).
- [23] A. Kaiser, H. H. Wensink, and H. Löwen, *Phys. Rev. Lett.* **108**, 268307 (2012).
- [24] C. Reichhardt and C. J. Olson Reichhardt, *Phys. Rev. E* **90**, 012701 (2014).
- [25] B. Bijmens and C. Maes, *J. Stat. Mech.* (2021) 033206.
- [26] O. Chepizhko and T. Franosch, *New J. Phys.* **22**, 073022 (2020).
- [27] G. Volpe and G. Volpe, *Proc. Natl. Acad. Sci. U.S.A.* **114**, 11350 (2017).
- [28] M. Zeitz and H. Stark, *Eur. Phys. J. E* **40**, 23 (2017).
- [29] T. Jakuszeit, O. A. Croze, and S. Bell, *Phys. Rev. E* **99**, 012610 (2019).
- [30] U. M. B. Marconi, A. Sarracino, C. Maggi, and A. Puglisi, *Phys. Rev. E* **96**, 032601 (2017).
- [31] L. Caprini, F. Cecconi, A. Puglisi, and A. Sarracino, *Soft Matter* **16**, 5431 (2020).
- [32] L. Caprini and U. M. B. Marconi, *Soft Matter* **14**, 9044 (2018).

- [33] F. Höfling and T. Franosch, *Rep. Prog. Phys.* **76**, 046602 (2013).
- [34] M. J. Saxton, *Biophys. J.* **52**, 989 (1987).
- [35] J. D. Schmit, E. Kamber, and J. Kondev, *Phys. Rev. Lett.* **102**, 218302 (2009).
- [36] N. Dorsaz, C. De Michele, F. Piazza, P. De Los Rios, G. Foffi, R. La, D. Fisica, and P. A. Moro, *Phys. Rev. Lett.* **105**, 120601 (2010).
- [37] K. Nakazato and K. Kitahara, *Prog. Theor. Phys.* **64**, 2261 (1980).
- [38] R. A. Tahir-Kheli and R. J. Elliott, *Phys. Rev. B* **27**, 844 (1983).
- [39] H. van Beijeren and R. Kutner, *Phys. Rev. Lett.* **55**, 238 (1985).
- [40] J. Reichert and T. Voigtmann, *Soft Matter* **17**, 10492 (2021).
- [41] T. Bertrand, Y. Zhao, O. Bénichou, J. Tailleur, and R. Voituriez, *Phys. Rev. Lett.* **120**, 198103 (2018).
- [42] R. Chatterjee, N. Segall, C. Merrigan, K. Ramola, B. Chakraborty, and Y. Shokef, *J. Chem. Phys.* **150**, 144508 (2019).
- [43] T. Chou, K. Mallick, and R. K. P. Zia, *Rep. Prog. Phys.* **74**, 116601 (2011).
- [44] K. Mallick, *Physica (Amsterdam)* **418A**, 17 (2015).
- [45] O. Bénichou, K. Lindenberg, and G. Oshanin, *Physica (Amsterdam)* **392A**, 3909 (2013).
- [46] v_0 is the analogous of the propulsion velocity in usual continuous-space models of active Brownian or run-and-tumble particles. Here, given that the particle evolves on a lattice, v_0 is bounded by $1/\tau$. Note that, given our choice of $p_\mu^{(\chi)}$, the active force \mathbf{F} controls v_0 but also controls the magnitude of the fluctuations in the direction perpendicular to \mathbf{F} .
- [47] See Supplemental Material at <http://link.aps.org/supplemental/10.1103/PhysRevLett.128.038001> for details of calculations and numerical simulations.
- [48] Note that the calculation of D requires the calculation of X_χ^∞ —the average position of the tracer conditioned on state χ in the stationary state—whose expression is given in the Supplemental Material [47].
- [49] O. Bénichou, P. Illien, G. Oshanin, A. Sarracino, and R. Voituriez, *Phys. Rev. Lett.* **113**, 268002 (2014).
- [50] P. Illien, O. Bénichou, G. Oshanin, A. Sarracino, and R. Voituriez, *Phys. Rev. Lett.* **120**, 200606 (2018).
- [51] O. Benichou, P. Illien, G. Oshanin, A. Sarracino, and R. Voituriez, *J. Phys. Condens. Matter* **30**, 443001 (2018).
- [52] T. Bertrand, P. Illien, O. Bénichou, and R. Voituriez, *New J. Phys.* **20**, 113045 (2018).
- [53] C. Lozano, J. R. Gomez-Solano, and C. Bechinger, *Nat. Mater.* **18**, 1118 (2019).
- [54] S. Leitmann and T. Franosch, *Phys. Rev. Lett.* **111**, 190603 (2013).
- [55] S. Leitmann and T. Franosch, *Phys. Rev. Lett.* **118**, 018001 (2017).
- [56] M. J. A. M. Brummelhuis and H. J. Hilhorst, *Physica (Amsterdam)* **156A**, 575 (1989).
- [57] O. Bénichou and G. Oshanin, *Phys. Rev. E* **66**, 031101 (2002).
- [58] P. Illien, O. Bénichou, C. Mejía-Monasterio, G. Oshanin, and R. Voituriez, *Phys. Rev. Lett.* **111**, 038102 (2013).
- [59] O. Bénichou, A. Bodrova, D. Chakraborty, P. Illien, A. Law, C. Mejía-Monasterio, G. Oshanin, and R. Voituriez, *Phys. Rev. Lett.* **111**, 260601 (2013).
- [60] P. Illien, O. Bénichou, G. Oshanin, and R. Voituriez, *Phys. Rev. Lett.* **113**, 030603 (2014).
- [61] O. A. Croze, G. P. Ferguson, M. E. Cates, and W. C. Poon, *Biophys. J.* **101**, 525 (2011).